CONTEXTUAL ARTIFICIAL INTELLIGENCE FOR ELECTRIC VEHICLE ROUTING WITH MOBILE WIRELESS CHARGING 3 4 5 6 Gyugeun Yoon, Ph.D. 7 Postdoctoral Associate 8 Department of Agribusiness, Applied Economics and Agriscience Education 9 North Carolina A&T State University, Greensboro, NC 27411 10 Email: gyoon@ncat.edu 11 ORCiD: 0000-0003-1622-9021 12 13 **Hyoshin Park, Ph.D.** 14 Associate Professor 15 Department of Engineering Management and Systems Engineering 16 Old Dominion University, Norfolk, VA 23529 17 Email: h1park@odu.edu 18 ORCiD: 0000-0002-1490-5404 19 20 Venktesh Pandey, Ph.D. 21 Assistant Professor 22 Department of Civil, Architectural, and Environmental Engineering 23 North Carolina A&T State University, Greensboro, NC 27411 24 Email: vpandey@ncat.edu 25 ORCiD: 0000-0003-0213-702X 26 27 Word Count: $4003 \text{ words} + 2 \text{ table(s)} \times 250 = 4503 \text{ words}$ 28 29 30 31 32 33 34

35 Submission Date: August 2, 2023

1 ABSTRACT

As more drivers have switched to electric vehicles (EVs), there has been higher interest in installing EV charging infrastructure. While most operators have focused on locating stationary charging stations (SCSs), several ideas have been proposed to implement wireless charging systems without direct connections. Among different types of systems, mobile energy distributors (MEDs) can provide the highest flexibility since it does not require massive construction. If both systems become available to drivers, they will make decisions on routes that may include SCSs or MEDs, considering total travel time, state of charge, wait time and cost for charging, and other factors. This study proposes a decision-making support system for EV drivers by reviewing the contexts of given route options. The system 1) extracts feasible routes from the road network and 10 EV charging system, 2) evaluates the value of routes regarding estimated weights of factors, 3) 11 recommends the one with the highest value, and 4) observes and archives the drivers' responses to 12 recommendations. In an experiment with a small 3-by-3 grid network, the proposed system can suggest satisfactory routes 16.5-26.9 pp more than the reference recommendation policy. 14

15

16 Keywords: Electric vehicle, Contextual AI, Charging infrastructure, Route recommendation, Wire-

17 less charging

INTRODUCTION

Electric vehicles (EVs) have been spotlighted as an alternative to conventional internal combustion engine vehicles as they are independent of gasoline or diesel fill-up. During operations, they emit less or near-zero pollutants including greenhouse gases and particle matter. However, there have been controversies about the environmental sustainability of EVs originating from several concerns. For example, battery production may induce excessive exploitation of minerals such as lithium and other rare-earth materials, accompanied by severe earth and water pollution. Moreover, they may generate more particle matter due to the friction between road surfaces and tires with more substantial torque. Nevertheless, EVs are perceived as critical in relieving global warming by reducing emissions.

Global vehicle sales trend shows the recent popularity of EVs. In 2022, about 14% of new vehicles sold worldwide were EVs, exceeding 10 million (1). The market share has grown from around 5% in 2020 and around 9% in 2021, showing exponential growth. This explosive growth mainly results from individuals' interest in environment-friendly vehicles and governments' subsidies to supplement high prices due to batteries made of rare earth materials. In addition, customers expect to counter the initial vehicle cost with savings in operation cost, e.g. charging cost. Since an EV is a relatively novel technology and most of them recently started to hit the roads, they will be supported by various subsidies for a while until they can achieve economic feasibility. Although there are signals showing the dependence of EV demand on subsidies when phasing out them, it is expected that the unit production cost of EVs will fall along the technological advance and market maturation. To keep promoting EV sales, some regions like Europe decided to ban internal combustion engine vehicles (ICEVs) by 2035 (2).

Meanwhile, inconvenience caused during EV charging is one of the largest disadvantages of EVs compared to regular vehicles. Drivers concern not only about the relative scarcity of available charging stations but also the length of charging time. Especially, vehicles should stop longer at chargers when being charged than at gas pumps when being filled up. For example, while gas tanks of ICEVs can be full in 2 minutes (3), Tesla Superchargers, the fastest charging device provided to drivers, can charge 200 miles in 15 minutes, about half of their sedan, Model S (4). This additional time for charging "energy" from sources can make customers be reluctant to switch to EVs.

In consequence, numerous interests in charging infrastructure have been raised to relieve those concerned previously mentioned, attracting a vast number of researchers to study the allocation and operation of fixed charging infrastructure. Qiu and Du (5) recently studied an EV-to-EV charging system, excluding infrastructure from these interactions. Nevertheless, there are a limited number of studies that consider dynamic charging systems as serious alternatives to stationary charging systems (SCSs) because not only they are premature but also difficult to operate. For example, mobile energy distributors (MEDs) are similar to portable batteries After being connected to vehicles, they keep charging vehicles by following them along their travels.

Despite its immature technology and operational complexity, this study incorporates both SCS and dynamic charging systems at the same time. Specifically, it focuses on designing a policy to recommend optimal routes to EV drivers considering: 1) their current vehicle state such as remaining battery level, 2) individual preferences, and 3) network and charging infrastructure characteristics. This paper is structured as follows. First, a methodology is proposed to integrate both SCS and DCS into EV drivers' route choices after reviewing relevant literature. Third, a sample experiment is conducted to illustrate the performance of the applied designed methodology.

1 Consequently, the paper concludes with the expected benefit and limitations of the methodology.

2 METHODOLOGY

9

10

1112

13

14 15

17

19

21

23

2425

2627

28 29

30

3 Simple example of EV routing

- 4 Consider a simple transportation network with both static and dynamic charging infrastructures
- 5 with the link travel time (e.g., minutes), shown as numbers on them in Figure 1. The static charging
- 6 infrastructure has two SCSs at Nodes 3 and 4. For the dynamic charging infrastructure, MED is
- assumed to follow a predefined schedule departing every 30 minutes from depot M and traveling
- 8 along the given route (dashed line) (M)-2-5-6-(M).

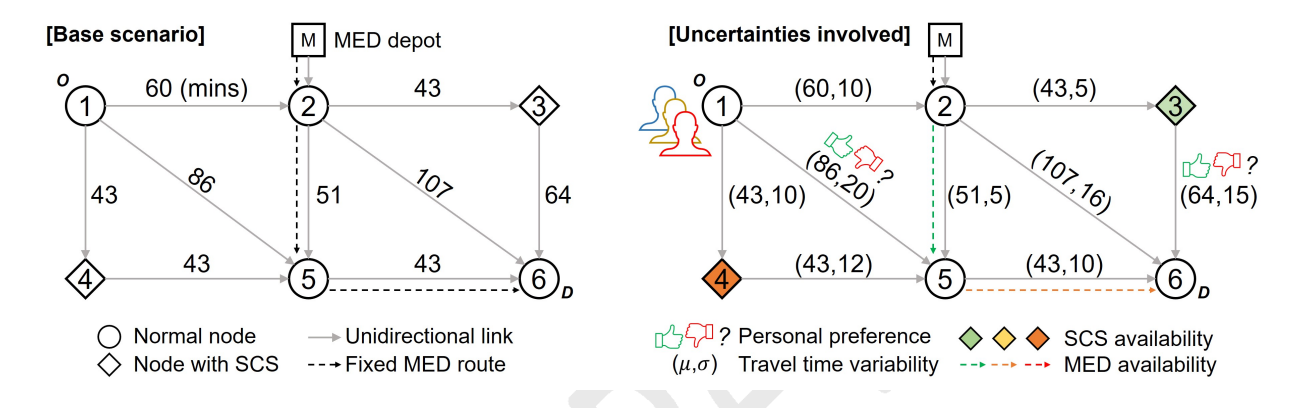


FIGURE 1 Base scenario and potential uncertainties.

If an EV driver should decide the shortest (travel time) path from origin O to destination D, the answer will differ depending on the initial state of charge (SoC). The en-route driver behaviors are influenced by the amount of energy available during the trip. For an EV with a 200-mile range and 50 kWh battery capacity, then in the deterministic case, the shortest path (1-5-6 and 1-4-5-6) consumes 37.5 kWh to reach D.

However, an initial SoC of 25 kWh is only sufficient for traveling to Node 5. Recharge is required either at the SCS at Node 4 (Route 1-4-5-6 only) or with the MED connectable at Node 5. For the SCS option (assuming a level 3 charger with a rating of 1 hr charge = 180 miles), at least 33 minutes of the minimum charge time requirement will be added to the travel time. On the other hand, if the EV driver instead uses MED at Node 5, the total travel time can be reduced as the EV connected with MED keeps moving while charging at an assumed speed of 80% of traffic flow speed. A 5.2 min of travel time savings is estimated when using MED (128.6+10.7=139.9 (min)) instead of charging at SCS (128.6+16.7=145.2 (min)). Furthermore, the driver may have to wait for the available charger or MED arrival and should tolerate longer travel time. SCS at node 3 is not be a feasible option for the EV with this initial SoC (i.e., 25 kWh), however, this path option and charging strategy (1-2-3-6) becomes feasible for EV with initial SoC of {38,50} kWh.

As a variation of the above problem, a certain level of unpredictability or randomness in E-VRP has been considered (6–8). The main objective of the literature has been optimizing travel distance/time and the fleet size constrained by vehicle weight capacity, time windows, station capacity, and tour duration limit. However, total energy consumption or recharging cost that may depend on the speed has been overlooked (9). The charging availability has been treated as negligible (10) only applied for private ownership of chargers. Only a few studies in the E-VRP context

10

11

13

15

17

20

21 22

23

26

considered charging availability in probabilistic model (11) or queuing model (12) driven from vehicle arrival interval and average service time.

As shown in Figure 2, temporal aspects of E-VRPSMC makes the above problem non-trivial. Depending on the departure time, the time-dependent travel time in each link generates different total cost of paths. Each EV driver would have different perspective on uncertainties in travel time and wait time/availability of SCSs and/or MEDs. Path uncertainties associated with SCSs may cause higher variability with lower mean, while MEDs would have less source of uncertainty by nature therefore lower variability. In this particular example, a risk-averse person may prefer charging with MEDs.

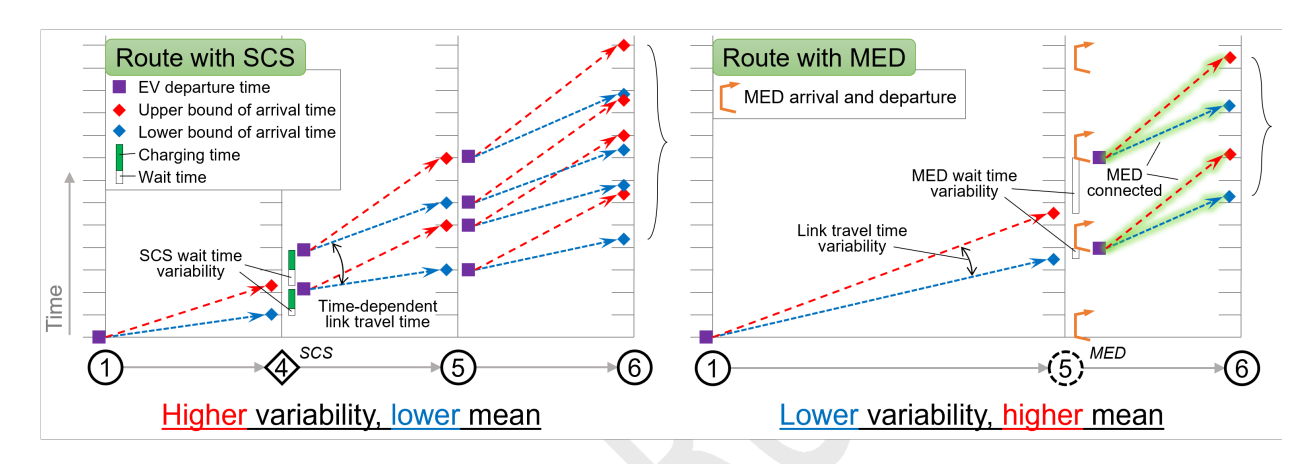


FIGURE 2 Illustrative example of the dynamics in a stochastic time dependent EV network

For this sequential EV route decision making problem under multiple sources of uncertainties (e.g., travel time, wait time, availability) in charging, in this study, we develop computationally efficient and explainable contextualized machine intelligence. The statistical profile of features and costs of each charging option will be analyzed and paired with driver preferences. The proposed transfer learning efficiently updates prior beliefs on charging in a sequence and the posterior inference will have lower uncertainty as more observations in those behaviors are available.

Problem statement

As shown in Figure 3, depending on the initially available network, vehicle, charging infrastructure, and network travel time information, the vehicle can decide which action to take: charge, wait, or move to the next node. Vehicle state and charging infrastructure information are updated corresponding to chosen actions. A session terminates when the battery is completely discharged or the vehicle arrives at the destination. The algorithm moves on to the next session with newly accumulated knowledge about the given situation.

For detailed formulation, a transportation network is considered as a graph network G = (N, L), where $n \in N$ is the set of nodes representing charging locations or intersections for directional changes and $l \in L$ is the set of links representing the roadway connection between the nodes. Each SCS $p \in P$ (where $P \subset N$) has uncertain availability (i.e. occupied by another vehicle), denoted by a random variable v_p . The EV can wait for a time interval W_p^{max} to charge if SCS p is unavailable ($v_p = 0$) on arrival. We define the expected waiting time at each p as $[1 - \Pr(v_p = 1)] * \overline{W}_p$, where \overline{W}_p is the average of waiting times ($E[W_p|v_p = 0]$) at p dependent on

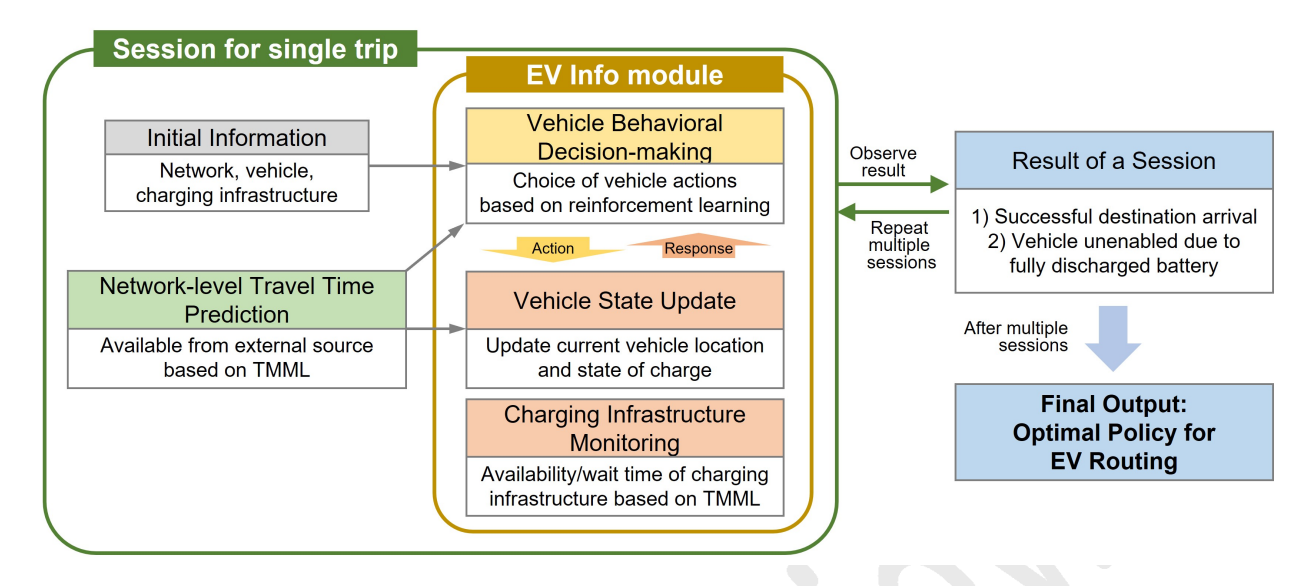


FIGURE 3 The Contextual AI framework for EV routing with wireless charging

- several parameters such as time of day. We note that $[1 \Pr(v_p = 1)]$ is zero when $\Pr(v_p = 1) = 1$.
- 2 To support the energy demands of EVs in the network, a set of MED $k \in K$ is provided for dy-
- namic charging services. Each MED k has a predefined schedule given by a sequence of stops
- 4 $S^k = (s_1^k, s_2^k, ..., s_M^k)$, and arrival time at those stops. The estimated EV waiting time arrived at k's stop s_m^k at time t is given as $W_k = t_m^k t$. The waiting time of EV is estimated based on advance
- 6 information on the availability of the MED at the given stop. The total cost measured in mone-
- tary units C_{total} is designed to be the sum of all costs: travel time C_{tt} , waiting time at charging
- 8 infrastructure C_{wt} , charging time C_{ct} , charging monetary C_{cm} , and energy consumption C_e .

$$C_{total} = C_{tt} + C_{wt} + C_{ct} + C_{cm} + C_{e}$$

$$= \omega_{tt} \sum_{(i,j)\in P} t_{ij} + \omega_{wt}(W_p + W_k) + \omega_{ct}(B_p + B_k) + (\delta_p c_p + \delta_k c_k) + \delta_e d_e$$
(1)

State space

14

15

16

17

The state space of the EV problem with SCS and MEDs for dynamic charging is represented by
$$\mathcal{S} = \left\{ \left(i, t, b_i, \operatorname{Av}_{\text{SCS}i=p}^t, \operatorname{Av}_{\text{MED}i=s_m^k}^t \right) : i \in N, b_i \in [0, Q_{\text{max}}], \operatorname{Av}_{\text{SCS}i} \in \{0, 1\}, \operatorname{Av}_{\text{MED}i} \in \{0, 1\} \right\}$$

- where i is the current location of the EV, t is the current time, b_i is the State of Charge (SoC) at current location, $Av_{SCS_n}^t$ is the availability of SCS at location i at current time t, and $Av_{MED_k}^t$ is the availability of MED at location i at current time t. The following scenarios are used to characterize 12 13 the terminal states (i.e., states that define the end of a learning episode)
 - Terminal states
 - if $e(t_{ij}, v) > b_i$, and waiting time at $i = \infty$ for $Av_{SCSi}/Av_{MEDi} = 0$ and $i \neq destination$: min reward.
 - if $b_i > 0$, and i = destination: max reward.
- Previous studies assumed the probability of a station being available and the expected wait-18 ing time when a station is unavailable to be independent of all external factors except for the station itself (11). However, in reality, these parameters could be influenced by multiple variables, such as

the time of day, the number of cars observed at the station, or previously observed availabilities at other stations that have been visited.

Incorporating the additional information (features) would cause the state space, decision policy, and algorithm computation time to increase exponentially due to the curse of dimensionality, making the models even more computationally difficult (13). For example, for each SCSp, the probability of availability ($Pr(Av_{SCSp} = 1)$) is dependent on factors such as time of day, number of EV observed at the station, or previously observed availabilities at other (visited/unvisited) SCS, weather, etc. (14–16).

 $Pr(Av_{SCSp} = 1 | Day, Time of day, No. of obs. EV, Prev. obs. avail., Weather).$

- 3 Action space
- 4 The actions at each current location consist of the possible links that can be traversed from the EVs
- 5 current location. The EV must satisfy the energy requirement for traversing the link or must use a
- 6 SCS or MED if available at the current location (i.e., i = p or s_m^k) to support its energy requirement:

$$\mathscr{A}_{(i,b_i)} = \left\{ (j,rc_i) : (i,j) \in E, rc_i \in RC_{ij}(b_i) \right\},\,$$

where each action consists of the next node j to visit, along with the amount of charge 7

- $rc_i > 0$ feasible at the current node if i = p or s_m^k . if $rc_i > 0$, then the EV must charge at current
- location i. This allows only the actions that will enable EV to reach the next node $(b_i \ge 0)$
- 10 EV SoC update
- 11 While the main contribution of this study is on optimal learning for EV routing, it's critical to
- 12 consider appropriate relationships between SoC and vehicle activities regarding wireless charging
- while driving. Folloing components are considered for sophisticated SoC updates.

We use a piecewise-linear EV battery charging function (17) $c(\hat{t}, b)$, depending on charging time \hat{t} and initial SoC level b. The function $c(\hat{t},b)$ accounts for the battery's reduced capability of absorbing energy when the SoC is high. Assuming the maximum EV charging rate is r, three sections have different charging rates: r in SoC of 0-85%, $\frac{r}{2}$ in 85-95%, and $\frac{r}{2}$ in 95-100%. For an empty battery (i.e., b = 0) and charging time \hat{t} , the SoC after charging (assuming that no energy is consumed while charging) is

$$\hat{c}(\hat{t}) = \min\{r_1 \hat{t}, 0.85Q + r_2(\hat{t} - t_1), 0.95Q + r_3(\hat{t} - t_2), Q\},$$
(2)

 $\hat{c}(\hat{t}) = \min\{r_1\hat{t}, 0.85Q + r_2(\hat{t} - t_1), 0.95Q + r_3(\hat{t} - t_2), Q\},$ 14 where $t_1 = \frac{0.85Q}{r_1}$ and $t_2 = t_1 + \frac{0.1Q}{r_2}$ are the first two breakpoints of the piecewise-linear, concave, and nondecreasing charging function. Q is the EV battery size.

We use a speed-dependent energy consumption model (18).

$$e(t,v) = t\left(\gamma_1 v + \gamma_2 v^3 + \gamma_3\right). \tag{3}$$

16 t is travel time, v for speed, and $\gamma_1, \gamma_2, \gamma_3$ are vehicle-specific constants: $\gamma_1 = \frac{g \cdot C_r \cdot m}{\eta}, \gamma_2 = \frac{C_w \cdot A_F \cdot \rho}{2 \cdot \eta},$ 17 and $\gamma_3 = P_0$ where g is gravity, C_r is rolling resistance, m is weight, η is engine efficiency, C_w is

drag coefficient, A_F is frontal surface area, ρ is air density (200 meters above sea level, temperature 18

 20° C), and P_0 is auxiliary power. 19

We use a dynamic charging/discharging model while driving (19) for EVs' SoC when it traverses link/arc $(i, j) \in E$. The model will estimate the SoC of the EV after it travels on link $(i, j) \in E$ either connected or unconnected to MED. To ensure longer charge duration, it is assumed

- that EV's reduce speed for dynamic charging on links/routes when connected to MED. The SoC
- $\beta(j,t_{ij},b_i)$ at location j, considering the travel time t_{ij} on link (i,j) and initial SoC b_i at current
- 25 location i is defined as

20

21

22

5

$$\beta(j,t_{ij},b_i) = \begin{cases} c(t_{ij},b_i) & \text{if EV is connected to MED for distance } d_a, \\ b_i - e(t_{ij},v) & \text{if EV traverses distance } d_a(unconnected), \text{ and } b_i - e(t_{ij},v) \geq 0, \end{cases}$$
 Note that $v = \frac{d_{ij}}{t_{ij}}$. Any scenario where $\beta(j,t_{ij},b_i) = b_{ij} - e(t_{ij},v) < 0$ is infeasible since battery lower limit is zero. In such cases, the link (i,j) can not be traversed by the EV unless it has been charged to a sufficient level. The total time of contact between a MED and EV is calculated according to the length of the road segment d_{ij} and the velocity(speed) of the MED, v_{med} .

$$\hat{tt} = \sum_{(i,j) \in P'} \frac{d_{ij}}{v_{med}}$$

P' is the shared path between MED and EV after the initial point of contact.

```
Algorithm 1 DRL for EV routing with DWC
```

```
1: Input: G = (N, E), destination n_d, learning rate \alpha
    Initialize replay memory D to capacity N
    Initialize action-value function Q with random weights \theta
    Initialize action-value function \hat{Q} with random weights \theta' = \theta
2: for each EV routing decision (number of episodes) do
         s_1 \leftarrow \{x_1\} and preprocessed sequence \phi_1 = \phi(s_1)

    initial state or feature vector

         for h = 1...H do
4:
              Select random node a_h \in A(s_h) with probability \varepsilon
5:
              Otherwise select a_h = \operatorname{argmax}_a Q(\phi(s_h), a; \theta)
6:
              Perform action a_h and observe reward r_h and new feature vector x_{h+1}
7:
8:
              Set s_{h+1} = s_h, a_h, x_{h+1} and preprocess \phi_{h+1} = \phi(s_{h+1})
              Store transition (\phi_h, a_h, r_h, \phi_{h+1}) in D
9:
              Sample random minibatch of memories (\phi_i, a_i, r_i, \phi_{i+1}) from D
10:
              if terminal at step j+1 then
11:
12:
              else
13:
                  y_i = r_i + \gamma \max_a \hat{Q}(\phi(s_{i+1}), a'; \theta')
14:
              end if
15:
                          > Train Neural Network with stored experiences to find optimal weights
             Calculate \nabla L(\theta) = \mathbb{E}_{\phi,a} \left[ (y_i - Q(\phi_i, a_i; \theta)) \nabla_{\theta} Q(\phi_i, a_i; \theta) \right]
                                                                                                 16:
              Update \theta \leftarrow \theta - \alpha \nabla L(\theta)
17:
              Reset \hat{Q} = Q every C steps
18:
         end for
19:
20: end for
```

- 6 Charging policy
- 7 Each EV can charge to a maximum charging capacity Q_{max} and the charge level can not drop
- 8 below zero. At the EVs current location i, the set of required and/or feasible charging amount
- 9 RC_{ij}(b_i), prior to traveling along link (i, j) is given as RC_{ij}(b_i) = [$(e(t_{ij}, v) b_i)^+, Q_{\text{max}} b_i$]. The
- 10 minimum required energy/charge amount to traverse link (i, j) is restricted to positive numbers

- 1 (i.e., $(e(t_{ij}, v) b_i) > 0$). When this amount is less or equal to zero, EVs can traverse link (i.j)
- 2 without charging. The maximum possible charging for each EV at the current location is given as
- 3 $Q_{\text{max}} b_i$, assuming that $e(t_{ij}, v) \leq Q_{\text{max}}$, for all $(i, j) \in E$.
- For scenarios where EVs are connected to MEDs to traverse link (i, j), the charging amount
- 5 is estimated using the by the non-linear charging function $c(t_{ij}, b_i)$.
- 6 Reward and solution approach
- 7 The reward function $r = \mathcal{R}(s, a, s')$ estimates to a scalar value when the state transitions into state
- 8 s' from state s after taking action a. The reward is utilized to update the weights in the solution.
- 9 For example, in convolutional neural networks, each weight can be updated through backpropa-
- 10 gation using action-driven rewards. The below algorithm shows black box-based deep RL as the
- 11 benchmark. The full paper will include both the black box approach and contextual AI approach
- 12 built upon previous work to identify a subset of more valuable factors to incorporate.
 - Once there is a new observation of wait and travel time in SCS and MEDs, the external module TMML will update the prior and approximate the posterior distribution.

15 NUMERICAL EXPERIMENT

13

25

26

2728

29

31

32 33

35

36

In the numerical experiment, a 3-by-3 grid network in Figure 4 is used, consisting of 9 nodes 16 and 14 links. It shares the same markers to indicate nodes with SCSs and MED stops. Numbers in shapes are node IDs, and those in parentheses are the mean and standard deviation of travel 18 time on links. For example, when traveling on the link connecting Node 1 and 2 would take 20 38.6 minutes on average, and the standard deviation of travel time is 6.6 minutes. Dashed links represent the direction of MED routes, and they have 1.2 times longer travel time compared to 21 normal links, considering the assumption of speed reduction due to the safety issue. In addition, 22 nodes with access to charging systems have superscripts and subscripts; and each indicates the 23 mean and standard deviation of wait time for chargers. 24

On this network, 8 unique routes can be observed for traveling from Node 1 to 9. However, there are 21 different routes available when counting the same route as different ones regarding the usage of charging systems. Table 1 illustrates the sequence of nodes and charging system usages of routes. For instance, when using Route 11 in the table, a vehicle will start from Node 1, visit Node 2, 5, and 8, and arrive at Node 9. It will use SCS at Node 5 and MED between Node 8 and 9. As a result, the goal of the policy is to pick a route out of 21 that can be accepted by the driver who has different sensitivity to various aspects.

In the experiment, three different drivers are assumed to travel between Node 1 and 9 and get recommendations from the system. Their responses to suggestions are archived to estimate their perspectives on different trip attributes. Each driver is recommended with random routes 100 times and with ones with the highest value for the next 900 times.

RESULT

- 37 The main output of this research is the identification of an optimal policy for individual EV routing.
- 38 With the route generated by the policy, drivers will have a higher probability to complete their trips
- 39 within a reasonable time and tolerable variability before their batteries are depleted. Under the
- 40 deterministic settings, the optimal route may be equivalent to the most cost-efficient one with the
- 41 lowest generalized cost integrating travel cost, charging cost, and value of wait time. In contrast, a
- 42 vehicle would be asked to follow a route with longer expected travel time and lower variability ac-

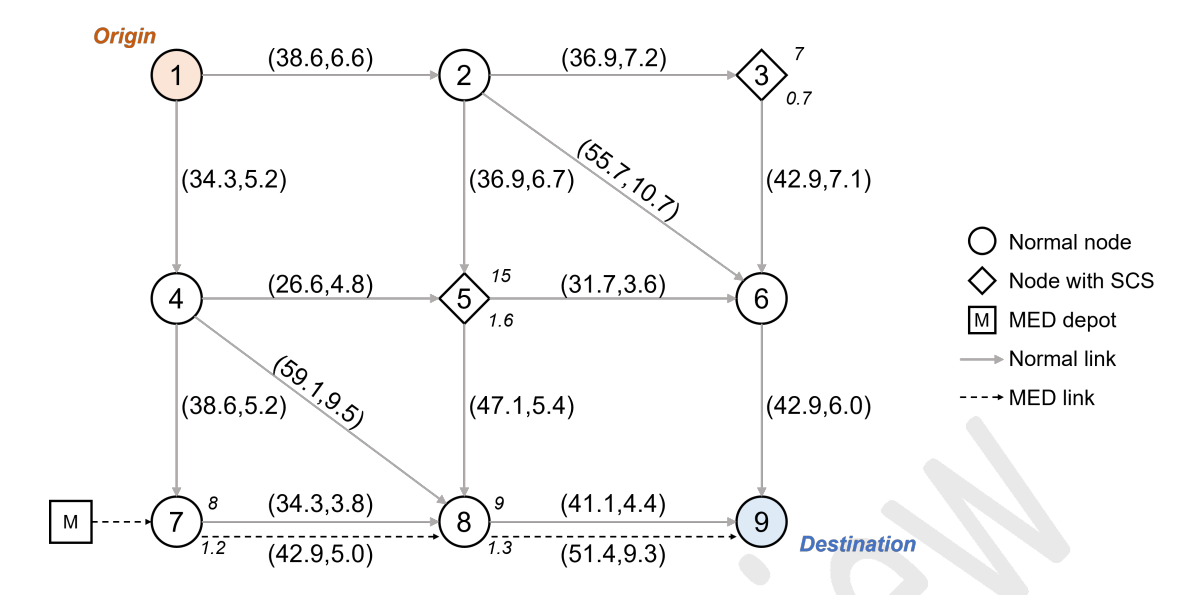


FIGURE 4 Sample network for numerical experiment

TABLE 1 Attributes of Enumerated Routes on Sample Network

Route #	Node Sequence	SCS usage	MED usage
1	1-2-6-9		
2	1-4-8-9		
3	1-4-8-9		8-9
4	1-2-3-6-9		
5	1-2-3-6-9	3	
6	1-2-5-6-9		
7	1-2-5-6-9	5	
8	1-2-5-8-9		
9	1-2-5-8-9	5	
10	1-2-5-8-9		8-9
11	1-2-5-8-9	5	8-9
12	1-4-5-6-9		
13	1-4-5-6-9	5	
14	1-4-5-8-9		
15	1-4-5-8-9	5	
16	1-4-5-8-9		8-9
17	1-4-5-8-9	5	8-9
18	1-4-7-8-9		
19	1-4-7-8-9		8-9
20	1-4-7-8-9		7-8
21	1-4-7-8-9		7-8,8-9

- cording to the driver's inclination. The more the system learns the situation, the better expectation
- 2 of successful completion of trips. After multiple times of observations, the system can estimate
- 3 parameters for evaluating routes.

7

11

12

13

15

16

17

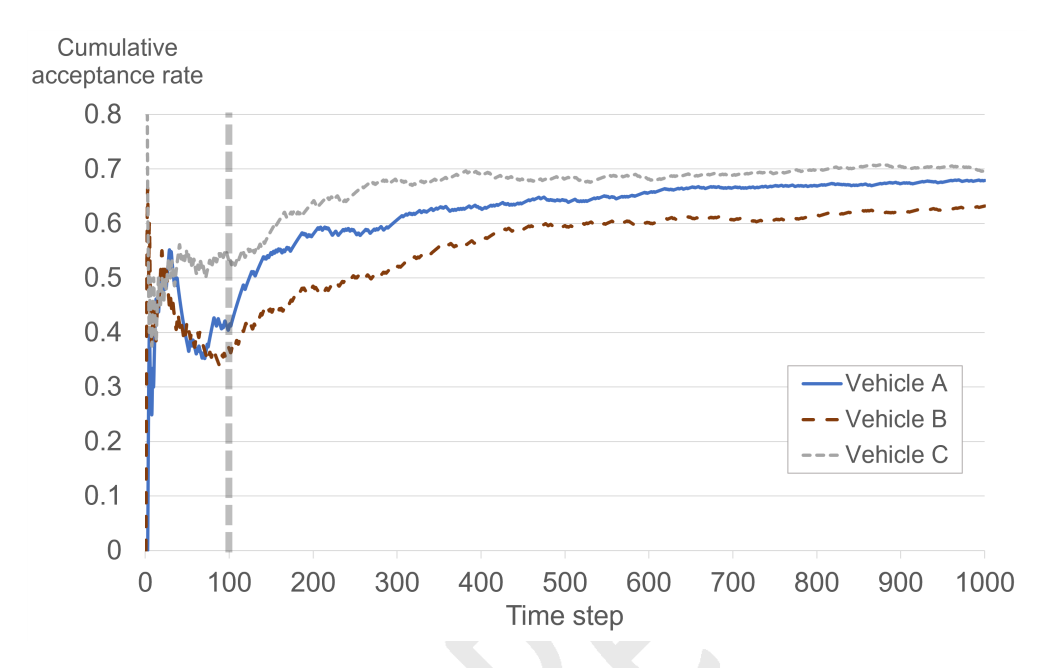


FIGURE 5 Sample illustration of expected result

The first result that represents the performance of the routing policy is the cumulative acceptance rate (see Yoon et al. (20)) and illustrated in Figure 5. First, operating a reinforcement learning-based routing algorithm in the numerical example will yield a sequence of choices and rewards. As the model continues to learn, its predictability for a successful route would be improved, leading to an asymptotically increasing cumulative acceptance rate. This enables the comparison of performance between the initial and mature models. In Figure 5, cumulative acceptance rate curves before the 100th time step are lower than plateaus near the 1000th time step respectively. By repeating the recommendation after collecting information from random route guidance, the algorithm can develop the model to increase the probability of recommending routes that can be accepted by the driver. Table 2 illustrates the extent of improvement per driver. Since all the given information including the network and the true parameters are artificially generated, the improvements shown in this figure may not reflect phenomena in the real world. Nevertheless, it shows evidence that the proposed algorithm can capture the direction of the policy which can increase the chance of recommending acceptable alternatives to users.

TABLE 2 Improvement of Cumulative Acceptance Rate by Vehicle

Vehicle	Rate at 100th	Rate at 1000th	Increment
A	41%	67.9%	26.9 pp
В	37%	63.2%	26.2 pp
C	53%	69.5%	16.5 pp

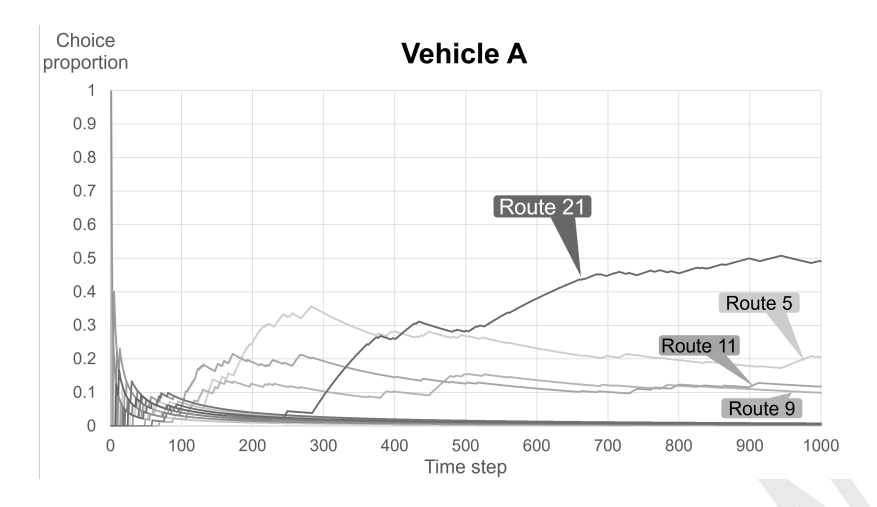


FIGURE 6 Cumulative route choice rate of Vehicle A

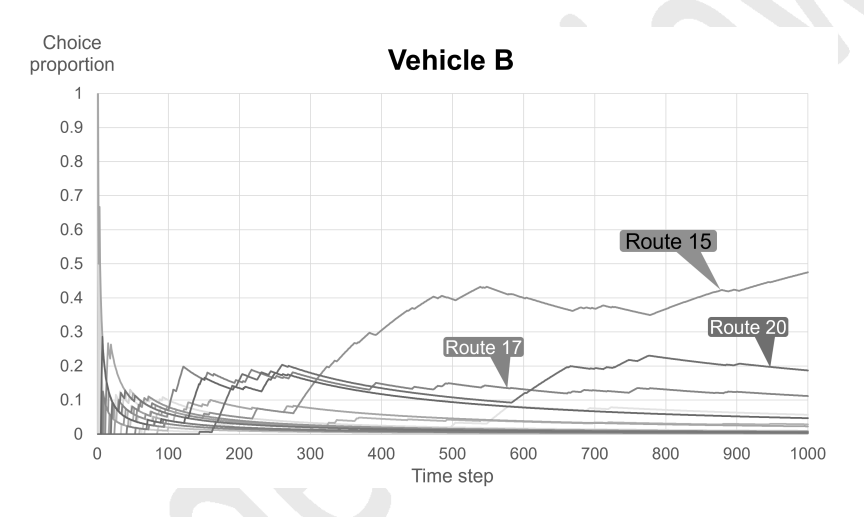


FIGURE 7 Cumulative route choice rate of Vehicle B

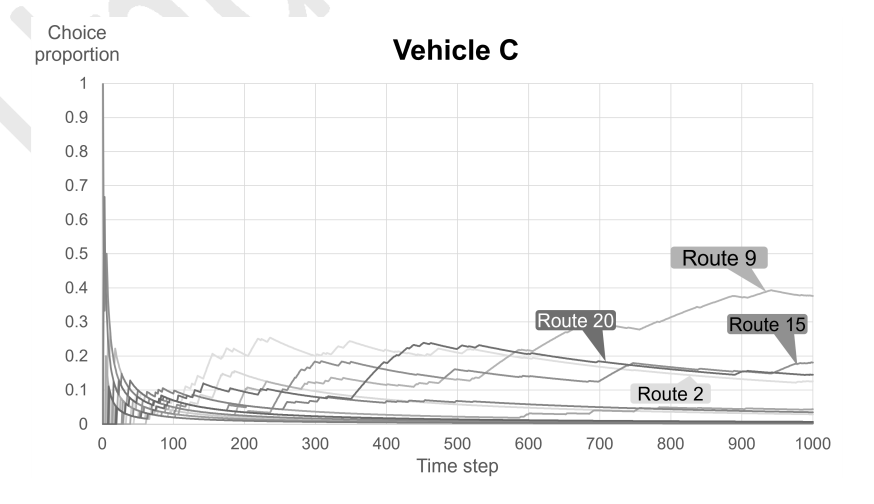


FIGURE 8 Cumulative route choice rate of Vehicle C

7

8

10

11

12

15

17

18

19

20 21

24

25

26

27

28

Secondly, the system can track the trend of choices made over routes to provide insights to users. In Figure 6, 7, and 8, curves represent the proportion of time steps that recommended the specific route. For example, in Figure 6, Route 21 was constantly recommended to the driver, followed by Route 5, 11, and 9. Since different true parameters are assigned to drivers, the result varies by vehicle. The origin of these differences can be found in Table 1. This historical information can be useful if the system should switch to the offline setting due to an emergency such as the failure of a component.

There can be some other results that can be derived such as significant factors influencing the routing the most. It seems to be possible to observe the extent of the impact of numerous factors and identify which one becomes more influential. After sufficient choice instances, the model can develop a set of parameters representing the effect of corresponding features. Nevertheless, due to a lack of real-world data, consideration of correlations among various factors was limited. This implies that the parameter estimation might not be accurate if comparing the assumed values and estimated ones. Therefore, it should be cautious to conclude the relationship and priority among factors.

6 CONCLUSION

This research provides a solution for EV routing that navigates drivers along a route with the highest value regarding travel time and cost, reliability, and charger availability if necessary. Despite the involved uncertainties, the algorithm based on reinforcement learning can identify the best action to choose by analyzing collected information.

The current design is for the individual EVs, but it can be expanded to the system level to enable the system-wide analysis for the evaluation of AI-based EV routing. If the algorithm can consider the social benefit during the routing, the system-level performance measures such as total mile-traveled can be compared between "greedy" and "altruistic" scenarios.

Moreover, one of future studies can concentrate on the optimization of wireless charging systems to respond to uncertainties from the user side such as sudden crowdedness. The result of this study can support the simulation structure of user groups, and the strategy of the operator can be validated by testing on that virtual environment.

29 ACKNOWLEDGEMENTS

- 30 Authors would like to acknowledge the support from NSF Grant No. 2106989, 2200590, and
- 31 1910397 that partially funded the research team.

32 AUTHOR CONTRIBUTION

- 33 The authors confirm contribution to the paper as follows: study conception and design: G.Y., H.P.,
- 34 V.P.; data collection: G.Y., H.P.; analysis and interpretation of results: G.Y., H.P.; draft manuscript
- 35 preparation: G.Y., H.P., V.P. All authors reviewed the results and approved the final version of the
- 36 manuscript.

1 **REFERENCES**

- International Energy Agency, Global EV Outlook 2023: Catching up with climate ambitions, 2023.
- 4 2. Dewan, A., EU lawmakers support banning gasoline car sales by 2035 in key vote.
- 5 https://www.cnn.com/2022/06/08/business/eu-climate-vote-energy-intl/ 6 index.html, 2022, accessed on 2023-07-30.
- 7 3. American Petroleum Institute, Staying Safe at the Pump. https://www.api.
- 8 org/oil-and-natural-gas/consumer-information/consumer-resources/
- 9 staying-safe-pump#: ``:text=It%20may%20be%20a%20temptation,be%
- 10 20discharged%20at%20the%20nozzle, 2021, accessed on 2023-07-30.
- 11 4. Tesla, Support: Charging Your Tesla. https://www.tesla.com/support/charging, 2023, accessed on 2023-07-30.
- 13 5. Qiu, J. and L. Du, Optimal dispatching of electric vehicles for providing charging on-14 demand service leveraging charging-on-the-move technology. *Transportation Research* 15 *Part C: Emerging Technologies*, Vol. 146, 2023, p. 103968.
- Lu, J., Y. Chen, J.-K. Hao, and R. He, The time-dependent electric vehicle routing problem: Model and solution. *Expert Systems with Applications*, Vol. 161, 2020, p. 113593.
- Wang, L., S. Gao, K. Wang, T. Li, L. Li, and Z. Chen, Time-dependent electric vehicle routing problem with time windows and path flexibility. *Journal of Advanced Transportation*, Vol. 2020, 2020.
- 21 8. Zhang, R., J. Guo, and J. Wang, A time-dependent electric vehicle routing problem with congestion tolls. *IEEE Transactions on Engineering Management*, 2020.
- 9. Kucukoglu, I., R. Dewil, and D. Cattrysse, The electric vehicle routing problem and its variations: A literature review. *Computers & Industrial Engineering*, Vol. 161, 2021, p. 107650.
- Froger, A., J. E. Mendoza, O. Jabali, and G. Laporte, Improved formulations and algorithmic components for the electric vehicle routing problem with nonlinear charging functions.

 Computers & Operations Research, Vol. 104, 2019, pp. 256–294.
- Sweda, T. M., I. S. Dolinskaya, and D. Klabjan, Adaptive routing and recharging policies for electric vehicles. *Transportation Science*, Vol. 51, No. 4, 2017, pp. 1326–1348.
- Keskin, M., G. Laporte, and B. Çatay, Electric vehicle routing problem with timedependent waiting times at recharging stations. *Computers & Operations Research*, Vol. 107, 2019, pp. 77–94.
- Powell, W. B., *Approximate Dynamic Programming: Solving the curses of dimensionality*,
 Vol. 703. John Wiley & Sons, 2007.
- Ma, T.-Y. and S. Faye, Multistep electric vehicle charging station occupancy prediction using hybrid LSTM neural networks. *Energy*, Vol. 244, 2022, p. 123217.
- Hecht, C., J. Figgener, and D. U. Sauer, Predicting Electric Vehicle Charging Station Availability Using Ensemble Machine Learning. *Energies*, Vol. 14, No. 23, 2021, p. 7834.
- 40 16. Su, S., Y. Li, Q. Chen, M. Xia, K. Yamashita, and J. Jurasz, Operating Status Prediction
 41 Model at EV Charging Stations with Fusing Spatiotemporal Graph Convolutional Net42 work. *IEEE Transactions on Transportation Electrification*, 2022.
- Montoya, A., C. Guéret, J. E. Mendoza, and J. G. Villegas, The electric vehicle routing problem with nonlinear charging function. *Transportation Research Part B: Methodologi- cal*, Vol. 103, 2017, pp. 87–110.

- 1 18. Asamer, J., A. Graser, B. Heilmann, and M. Ruthmair, Sensitivity analysis for energy demand estimation of electric vehicles. *Transportation Research Part D: Transport and Environment*, Vol. 46, 2016, pp. 182–199.
- Fernández, E., M. Leitner, I. Ljubić, and M. Ruthmair, Arc routing with electric vehicles: dynamic charging and speed-dependent energy consumption. *Transportation Science*, 2022.
- Yoon, G., J. Y. Chow, A. Dmitriyeva, and D. Fay, Effect of Routing Constraints on Learning Efficiency of Destination Recommender Systems in Mobility-on-Demand Services.
- 9 *IEEE Transactions on Intelligent Transportation Systems*, Vol. 23, No. 5, 2022, pp. 4021–10 4036.